Sustainable Food Technology

ROYAL SOCIETY OF CHEMISTRY

PAPER

View Article Online
View Journal | View Issue

Cite this: *Sustainable Food Technol.*, 2026, 4, 3239

Unlocking the potential of cysteine–xylose Maillard reaction intermediates as natural flavor precursors: a comprehensive study on flavor regulation, storage stability, and antioxidant activity

Di Kang,[b] Lin Jiang,[a] Songjin Zheng,[b] Yuan Hu,[a] Haifeng Wang,[a] Teng Li,[a] Yuying Fu *[a] and Yun Zhai *[a]

2-Threityl-thiazolidine-4-carboxylic acid (TTCA) and Amadori rearrangement products (ARPs), intermediates of a cysteine–xylose (Cys–Xyl) Maillard reaction system, have been proven to form desirable flavors during thermal processing. The results showed that both TTCA and ARPs revealed excellent environmental stability at low temperatures (≤25 °C), neutral pH (7), and low water activity (0.113). Under storage conditions of 40 °C, pH 9, and 0.843 water activity, the loss rates of TTCA and ARPs reached 7.06% and 12.17%, 11.19% and 21.25% and 35.77% and 60.61%, respectively. Further research found that TTCA and ARP have increased Fe^{2+} chelating ability, ferric ion reducing capacity, and free radical scavenging ability within a concentration range of 0.5 to 3.0 mg mL^{-1}. Additionally, different heat treatment conditions as well as the addition of different exogenous amino acids could regulate the flavor formation profile and characteristics of TTCA, making it suitable for different real food systems and broadening its processing adaptability. In particular, when the pH was increased from 5.5 to 8, the meaty flavor of the system gradually lightened, while flavor characteristics such as popcorn flavor, burnt flavor, and nutty flavor gradually strengthened. This research explored the potential of MRIs, natural flavor precursors, to serve as supplements and partial alternatives to synthetic additives. These findings provide a theoretical basis for developing more sustainable food systems and may help reduce the environmental footprint of food processing.

Received 5th December 2025
Accepted 10th March 2026

DOI: 10.1039/d5fb00932d

rsc.li/susfoodtech

Sustainability spotlight

In the context of a growing global pursuit of sustainable food systems, the development of natural, efficient flavor precursors and antioxidants has become a critical direction for the food industry. The use of TTCA/ARPs as natural flavor precursors and antioxidants can contribute to: (1) reducing reliance on synthetic additives, supporting cleaner labels and potentially lowering the environmental burden associated with chemical synthesis; (2) minimizing food waste through enhanced product stability and extended shelf-life; and (3) optimizing energy efficiency in food processing, as flavor formation can be regulated under varied, potentially milder thermal conditions. Utilizing natural and renewable precursors (cysteine and xylose) in a value-added reaction process.

1 Introduction

In the context of a growing global pursuit of sustainable food systems, the development of natural and efficient additives has become a critical direction for the food industry. Maillard reaction intermediates (MRIs) and Amadori/Heyns rearrangement compounds (ARPs/HRPs), which are naturally derived, hold significant potential as clean-label alternatives to synthetic flavor precursors and antioxidants.[1,2] Compared to the complex and variable nature of complete Maillard reaction products (MRPs), MRIs provide a stable and controllable source for generating ideal flavor and color upon thermal processing.[3] In particular, the Cys–Xyl system yields both the conventional ARP and a unique thiazolidine derivative, TTCA.[4,5] Current studies have investigated the fundamental aspects of TTCA and ARPs,[6,7] including their aqueous-phase tracing preparation mechanism, characteristic patterns of flavor formation and yield enhancement.[8,9] These investigations preliminarily demonstrate their advantages in controlled flavor formation, underscoring their potential as flavor precursors.

Existing studies confirm that the flavor intensity in thermally processed MRIs exhibits significant advantages; however, the profile of characteristic volatile compounds generated from

[a]*School of Food Science and Biotechnology, Zhejiang Gongshang University, Hangzhou, 310018, People's Republic of China. E-mail: 18352538819@163.com; webfu@126.com; wangmumu542@163.com; 15125949093@163.com; whf4341514@163.com; tli0718@mail.zjgsu.edu.cn*

[b]*China Tobacco Hebei Industrial Co., Ltd, Shijiazhuang, 050051, People's Republic of China. E-mail: 1283201616@qq.com; zsj211@126.com*

MRIs remains less diverse than that of the volatile compounds derived from MRPs.[8,9] Although adjusting the reaction parameters is a common regulatory approach, its ability to fully compensate for the lack of flavor complexity may be limited.[10–13] The addition of exogenous amino acids presents a promising alternative for modulating the flavor, which could promote Strecker degradation between regenerated amino acids derived from MRI degradation and dicarbonyl compounds to form a characteristic flavor.[14,15] Nevertheless, the systematic effect of different exogenous amino acids on the flavor profiles derived from specific intermediates, such as TTCA/ARP, remains unclear. Moreover, comprehensive approaches for regulating the flavor profile of TTCA/ARP are currently lacking. Besides, to enable flavor formation exclusively during subsequent thermal processing, MRIs must maintain stability during storage.[16] However, MRIs can further degrade through rearrangement and condensation pathways.[17,18] Thus, understanding their behavior during storage and heating is essential for commercial applications. Concurrently, developing natural antioxidants is crucial for food preservation.[19–21] MRPs exhibit confirmed antioxidant, antiallergic, and antibacterial activities,[22–24] primarily due to the presence of the chromophoric rings of melanoidins.[22,25] Certain low-molecular-weight compounds in MRPs, especially reductones and heterocycles, exhibit a greater antioxidant activity than pure melanoidins.[19] However, the specific contribution and efficacy of defined intermediate compounds like TTCA and ARPs have not been comparatively evaluated against MRPs.

Therefore, to address the current research gap regarding TTCA and ARPs, this study adopts a unique perspective to investigate the regulatory mechanisms of their flavor characteristics, storage stability, and antioxidant properties and aims to comprehensively evaluate the dual-function potential of TTCA and ARPs as flavor precursors and antioxidants through the following steps: (1) systematic assessment of the storage stability of TTCA and ARPs under different environmental stresses to provide essential data for their commercial storage; (2) elucidation of the directional regulation of the thermal degradation flavor profiles of TTCA by temperature, pH, and various exogenous amino acids to extend their processing adaptability; and (3) evaluation and comparison of the *in vitro* antioxidant activities of TTCA/ARPs with those of MRPs to clarify their roles and potential in different antioxidant pathways. Hence, this work provides essential data for the commercial storage and application of TTCA/ARPs, extends their processing adaptability, and clarifies their dual-function potential as natural flavor precursors and potential antioxidants, thereby supporting their development as sustainable food additives.

2 Materials and methods

2.1 Chemicals

Analytical grade L-cysteine, D-xylose, sodium hydroxide, 1,2,4-benzenetriol, phenanthroline, potassium ferricyanide, trichloroacetic acid, $FeCl_3$, DPPH, ethanol, 1,10-phenanthroline, $FeSO_4$, ascorbic acid, lecithin, thiobarbituric acid, H_2O_2, NaOH and HCl were purchased from Sigma-Aldrich Chemical Co. (Shanghai, China). LC-MS-grade water, acetonitrile, deuteroxide ammonium formate and 1,2-dichlorobenzene were purchased from Sinopharm Chemical Reagent Co. Ltd (Shanghai, China).

2.1.1 Accession codes. D-Xylose (PubChem CID: 135191); L-cysteine (PubChem CID: 5862); acetonitrile (PubChem CID: 6342); methanol (PubChem CID: 887); deuteroxide (PubChem CID: 24602); and ammonium formate (PubChem CID: 10904).

2.2 Synthesis, purification and characterization of isomeric TTCA and ARPs

The preparation, purification and characterization of TTCA and ARPs were carried out by following the methods reported in our previous studies.[4,26] An equimolar solution of Cys and Xyl (0.0827 mol L^{-1}) was prepared using deionized water. The prepared solution was maintained at pH 7.4 ± 0.01 using NaOH (6 mol L^{-1}), followed by the heat treatment for 40 min at 90 °C. The reaction vessel was quickly transferred to an ice-bath to terminate the reaction immediately. The obtained reactant was employed to examine the purity of TTCA and ARPs, which were preliminarily separated using an ion exchange resin (H^+ Dowex 50WX4, 200–400 mesh, Acros Organics, SERVA, J&K, Beijing, China) with ammonium hydroxide (0.2 mol L^{-1}) as the eluent, and further purification was carried out using a semi-preparative RP-HPLC equipped with an Xbridge Amide column (4.6 mm × 150 mm, 3.5 μm; Waters Co., Milford, MA, USA). The identification and characterization of TTCA and ARP purities were performed using UPLC-ESI-MS (Waters Synapt MALDI Q-TOF MS, USA) and NMR (Bruker DRX 400 MHz spectrometer). The specific procedures of the above-mentioned methods were accomplished by referring to our published study. The mass spectral and NMR spectral information is listed in the SI (Fig. S1 and Table S1).

2.3 Assessment of the browning index of the Maillard reaction solution

To assess the browning degree of the melamine reaction solution at different temperatures, the absorbance at 420 nm (A_{420}) was typically measured using a UV-visible spectrophotometer, which served as the browning index. The absorbance was determined by diluting the sample appropriately so that the A_{420} value was within a reasonable range (0.05 to 1.0).

2.4 Construction of the Maillard thermal reaction model system using TTCA as the base material

Maillard thermal reaction model systems were established with TTCA as the base material. The pH of the TTCA solution (10 mmol L^{-1}) was adjusted to 5.5, 7, and 8, respectively, using NaOH (6 mol L^{-1}). The prepared samples were then treated at different temperatures (100 °C, 120 °C, and 140 °C) for 120 minutes.

Additionally, an equimolar amount of different exogenous amino acids (Gly, Ala, Met, Leu, Ser, Thr, Pro, Val, Phe, His, Lys, Glu, and Asp) were added to the TTCA solution (10 mmol L^{-1}). The pH of the system was adjusted to 7.0 using NaOH

(6 mol L^{-1}), and the thermal reaction was conducted at 120 °C for 120 minutes.

Using high-temperature/high-pressure-resistant glass reaction vessels set in an oil bath, the aforementioned thermal reactions were carried out. Following this, all the mixtures were immediately transferred to an ice bath to halt the reactions. Afterwards, the samples were collected and kept under 4 °C for further analysis.

2.5 Determination of the storage stability of TTCA and ARPs

To investigate the effect of different storage temperatures on the stability of TTCA and ARP intermediates in solid and solution forms, a solid pure lyophilized powder of TTCA and ARPs was placed in self-sealing bags or dissolved in deionized water and configured as a solution with a concentration of 100 mmol L^{-1}, and placed in the ambient temperatures of 4 °C, 25 °C and 40 °C. The changes in concentration, A_{420}, A_{294}, and color were recorded every 10 days during storage, and storage stability was investigated over a period of 60 days.

In addition, the storage stability of the TTCA and ARP system was observed by varying the pH of the system while maintaining the same ambient temperature, and the same metrics were also examined. For TTCA and ARP solid samples, the effect of ambient humidity on their storage stability was investigated. A fixed mass of the dried powder of the intermediate was taken in an open glass Petri dish and transferred to a sealed desiccator, the bottom of which was filled with different saturated salt solutions configured to maintain the ambient moisture activity of the system, and a comparison of the moisture activities of different saturated salt solutions at 25 °C is shown in Table S2.

2.6 Determination of the antioxidant properties of intermediates

2.6.1 Measurement of the Fe^{2+} chelating capacity. The determination of the Fe^{2+} chelating capacity was conducted based on a previously established method.[27] First, 1 mL of sample was combined with 1.85 mL of deionized water, followed by the addition of 0.05 mL of $FeCl_2$ phenanthroline solution (5 mmol L^{-1}). After standing at 28 °C for 30 seconds, the mixture was allowed to react for an additional 10 minutes at the same temperature. It was then centrifuged at 3000 rpm for 5 minutes. The absorbance of the supernatant was measured at 562 nm using a UV-vis spectrophotometer. A blank control was prepared by replacing the sample with deionized water and analyzed identically. The chelating capacity was calculated using the following formula:

$$Fe^{2+}\ \text{chelation rate} = \frac{A_0 - A_1}{A_0} \times 100\%$$

where A_0 and A_1 are the absorbance of the blank and sample, respectively.

2.6.2 Measurement of the reducing power. The assay was initiated by mixing 1 mL of sample solution with 2.5 mL of phosphate buffer (pH 6.6) and 2.5 mL of 1% potassium ferricyanide solution. The resulting mixture was incubated in a 50 °C water bath for 20 minutes, followed by the addition of 2.5 mL of 10% trichloroacetic acid. After centrifugation at 3000 rpm for 10 minutes, 2.5 mL of the supernatant was collected and combined with 2.5 mL of 0.1% $FeCl_3$ solution and 2.5 mL of deionized water. Following a 10 minute reaction period, the absorbance at 700 nm (A_{700}) was measured using a UV-vis spectrophotometer to indicate the sample's reducing power.[28]

2.6.3 Measurement of the DPPH free radical scavenging capacity. The assay was initiated by combining 3 mL of 100 μmol L^{-1} DPPH ethanol solution with 1 mL of the sample. The mixture was then incubated in the dark at room temperature for 25 minutes. Its absorbance at 517 nm (A_i) was measured using a UV-visible spectrophotometer, with ethanol serving as the blank. Similarly, the absorbance of a control mixture containing 1 mL of ethanol and 3 mL of DPPH solution was recorded as A_0. Additionally, a sample background absorbance (A_j) was obtained by measuring a mixture of 1 mL of sample and 3 mL of ethanol. The DPPH radical scavenging capacity was calculated using the following formula:

$$\text{DPPH}^{\cdot}\ \text{clearance rate} = \left(1 - \frac{A_i - A_j}{A_0}\right) \times 100\%$$

2.6.4 Measurement of the hydroxyl radical scavenging capacity. For the assay, 1 mL of 2.5 mmol L^{-1} 1,10-phenanthroline was combined sequentially with 2 mL of phosphate buffer (pH 7.40), 1 mL of 2.5 mmol L^{-1} $FeSO_4$ solution, 1 mL of deionized water, and 1 mL of 20 mmol L^{-1} H_2O_2. Following 60 minutes of incubation at 37 °C in a water bath, the absorbance of the mixture at 536 nm was recorded immediately using a UV-vis spectrophotometer. The scavenging capacity against hydroxyl radicals was calculated using the following formula:

$$^{\cdot}\text{OH}\ \text{clearance rate} = \frac{A_s - A_1}{A_0 - A_1} \times 100\%$$

where A_S represents the absorbance of the sample; A_1 denotes the absorbance of the control reaction solution, which contains 1,10-phenanthroline, $FeSO_4$ and H_2O_2; and A_0 corresponds to the absorbance of the blank solution, composed solely of $FeSO_4$ and 1,10-phenanthroline.[7]

2.6.5 Measurement of the superoxide anion radical scavenging capacity. The method is grounded in the principle that antioxidants bind to superoxide anion radicals, forming stable species and thereby terminating the radical chain reaction, which releases chromogenic products. According to this principle, 9 mL of 50 mmol L^{-1} Tris–HCl buffer (pH 8.2) was combined with 0.5 mL sample and incubated in a water bath at 25 °C for 20 minutes. Immediately after that, 0.04 mL of a pre-warmed (25 °C) 1,2,4-benzenetriol solution (prepared by dissolving 0.45 mmol of 1,2,4-benzenetriol in 10 mL of 10 mmol L^{-1} hydrochloric acid) was added. After a 3 minute standing period, one drop of 10 mmol L^{-1} ascorbic acid solution was introduced. Following an additional 5 minute incubation period, the mixture's absorbance at 327.2 nm (A_{327}) was measured using a UV-vis spectrophotometer. The superoxide anion radical scavenging capacity was calculated using the following formula:

$$O_2^{\cdot-} \text{ clearance rate} = \frac{A_0 - A_1}{A_0} \times 100\%$$

where A_0 represents A_{327} of the blank and A_1 represents A_{327} of the sample.[7]

2.6.6 Measurement of the lipid peroxidation inhibition capacity. A dispersion of 10.0 mg mL^{-1} lecithin (denoted S_1) was prepared in 0.01 mol L^{-1} phosphate buffer (pH 7.4) using a magnetic stirrer. Separately, solution S_2 was prepared by dissolving 15 g trichloroacetic acid, 0.37 g thiobarbituric acid, and 2 mL concentrated hydrochloric acid in deionized water, followed by dilution to a final volume of 100 mL. For the assay, 1.0 mL of S_1 was mixed sequentially with 1.0 mL of 400 μmol L^{-1} $FeCl_3$ solution, 1.0 mL of 400 μmol L^{-1} ascorbic acid solution, and 1.0 mL of sample solution. The mixture was incubated at 37 °C in a water bath for 60 minutes. Subsequently, 2.0 mL of S_2 was added, and the mixture was heated at 95 °C for 15 minutes. After cooling in an ice-water bath for 10 minutes and centrifugation, the absorbance at 532 nm (A_{532}) of the supernatant was measured using a UV-vis spectrophotometer. The lipid peroxidation inhibition rate was calculated as follows:

$$\text{Inhibition rate} = \frac{A_0 - A_1}{A_0} \times 100\%$$

where A_0 and A_1 denote the absorbance of the blank (deionized water as the substitute) and the sample, respectively.[7]

2.7 Identification and quantification of the characteristic volatile compounds

The analysis of volatile flavor compounds was performed using headspace solid-phase microextraction coupled with gas chromatography-mass spectrometry (HS-SPME-GC-MS). The sample solution (3 g) was added with 3 μL internal standard (1,2-dichlorobenzene, 0.018 μg μL^{-1} in methanol), which was then placed in a 20 mL headspace vial. The extraction and desorption procedures were carried out by following a previously published method,[15] employing a divinylbenzene/carboxen/polydimethylsiloxane (CAR/PDMS/DVB, 75 μm) SPME fiber. Compound separation and identification were achieved using an Agilent 7890B gas chromatograph interfaced with a 5977B mass selective detector. Following 10 minutes of thermal desorption at 250 °C in the injection port, the volatiles were transferred onto an analytical column. Chromatographic separation was performed using a 30 m DB-Wax capillary column (0.25 mm i.d. and 0.25 μm film thickness). Specific instrumental conditions were adopted from our previous research.[15]

Compound identification was based on matching the mass spectra against the NIST 17 and WILEY 07 databases, comparing the calculated Kovats retention indices (RI) with the values reported in the literature, and referencing literature data. To facilitate accurate RI matching, the retention indices of target compounds were calculated by analyzing a C_7–C_{30} *n*-alkane series under identical chromatographic conditions. For compounds with available reference standards, their contents were determined by the standard curve method with the internal standard calibration (see Table S3); for those without reference standards, quantification was performed just using the internal standard method.

2.8 Data analysis

We conducted all experiments in triplicate, and the data are presented as mean ± standard deviation. Data processing involved the following steps: (1) analysis using SPSS Statistics 22.0 and Microsoft Excel 2010 and (2) multiple comparisons *via* Duncan's multiple range test, where a *p*-value of less than 0.05 indicated statistical significance.

3 Results and discussion

3.1 Regulating the characteristic flavor formation of the TTCA intermediate through parameter regulation

Given the established similarity in flavor formation pathways between TTCA and ARP (differing primarily in rate), TTCA was selected to investigate the effects of temperature and pH. Temperature is a key kinetic parameter in controlling the reaction progress. The appropriate increase in temperature is beneficial for accelerating effective collisions between substrates and the thermal degradation of cysteine.[29] Comparative studying of heated TTCA models at 100 °C, 120 °C, and 140 °C revealed that the total volatile flavor substances increased markedly, with sulfur-containing compounds showing a leapfrog increase (Table S4 and Fig. 1a). The content of furfural (the dominant furan) increased significantly, reaching 11.039 μg L^{-1} at 140 °C, which was 3.3 times that at 100 °C. The concentrations of 2-methyl-3-furanthiol and 2-furfurylthiol also increased accordingly. This is because high temperatures promote the enolization of ARPs, leading to the rapid generation and accumulation of the direct precursors like 3-DX and 1-DX for furfural and 4-hydroxy-5-methyl-3(2*H*)-furanone (Fig. 1f).[30] They also increase the generation of furan and 2-methylfuran, which are precursors to thiophene compounds (Fig. 1f). Furthermore, elevated temperatures intensified the thermal degradation of TTCA and free Cys (Fig. S2 and S3), resulting in an increased release of H_2S. The boosted supply of these key precursors (α-dicarbonyls, furans, and H_2S) strengthened their interactions, thereby promoting the formation of corresponding thiols and thiophenes (Fig. 1f).

Key steps such as enolization, retro-aldolization, and Strecker degradation are pH-dependent, and the activity of key precursors like H_2S and NH_3 also varies with the pH values.[3] Therefore, the influence of different reaction pH values (5.5, 7, and 8) on the TTCA thermal reaction system was studied. The characteristic volatile compounds were predominantly sulfur-containing (Table S5). Under the acidic condition (pH 5.5), thiols were most abundant, followed by thiophenes; no nitrogen-containing heterocycles were detected. As the pH increased from 5.5 to 8, thiol and furan contents decreased, while thiazoles increased sharply to 10.952 μg L^{-1}. Notably, 2-acetylthiazole (nutty/popcorn odor) increased significantly with pH, comprising 27.01% of total thiazoles at pH 8. Pyrazines were detected only at pH 8 and 0.838 μg L^{-1}, a concentration much lower than that of sulfur-containing compounds. Post-

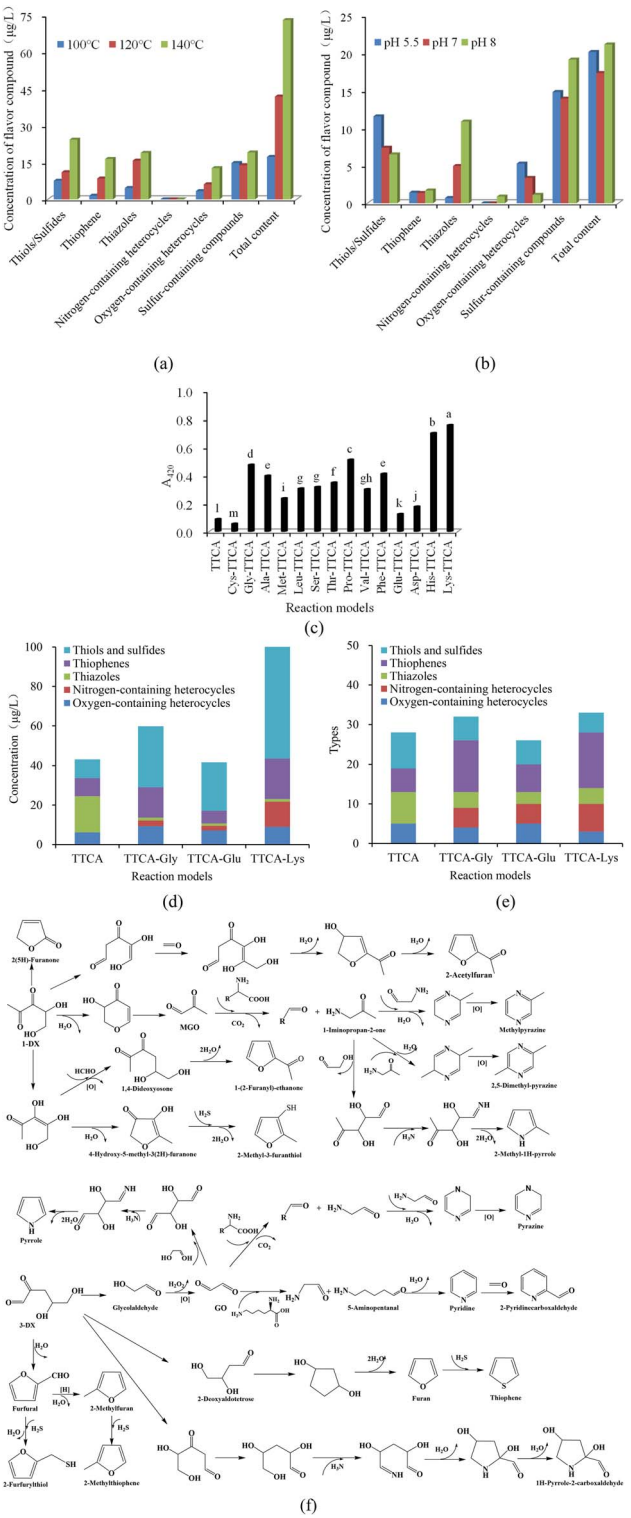

Fig. 1 Flavor formation from the TTCA model system under different conditions: (a) effect of temperature (100 °C, 120 °C, and 140 °C) at pH 7.0 on volatile compounds; (b) effect of pH (5.5, 7, and 8) at 120 °C on volatile compounds; (c) browning intensity of TTCA systems with different added amino acids; (d) contents and (e) types of characteristic flavor compounds from TTCA with Gly, Lys, or Glu; and (f) formation pathways for the characteristic flavor formation from TTCA with amino acids.

reaction, the system pH dropped (to 5.1, 4.9, and 4.7, respectively), due to organic acid formation from accelerated TTCA degradation at a higher initial pH. Under acidic conditions, TTCA undergoes 1,2-enolization, generating thiol and furan precursors (Fig. 1f).[15] The low thiazole and pyrazine contents under acidic conditions are due to the superior competitiveness of H_2S over NH_3/amines in capturing reactive α-dicarbonyl intermediates including glyoxal, methylglyoxal, and 2,3-butandione.[17] In contrast, alkaline conditions enhanced the nucleophilicity of deprotonated NH_3/amines, enabling them to successfully compete for intermediates and drive the formation of thiazoles and pyrazines, imparting roasted notes.[17] Alkaline conditions also favor the regeneration of Cys during TTCA degradation, promoting Strecker degradation with α-dicarbonyls and further amplifying thiazole/pyrazine formation (Fig. 1f).[3]

In summary, the increased temperature universally intensified flavor formation by elevating precursor supply and reaction rates. In contrast, the increased pH altered the fundamental reaction pathway, shifting the flavor profile from sulfur-rich/meaty notes toward nitrogen-containing heterocycles associated with the characteristics of roasted flavor. These findings confirmed that targeted parameter control (temperature and pH) can effectively steer the flavor formation pathways of TTCA, demonstrating its adaptable potential for generating diverse flavor profiles under different processing conditions.

3.2 Addition of exogenous amino acids regulating the formation of characteristic flavors of the TTCA reaction system

While TTCA intermediates produce intense flavors surpassing those of typical MRPs, their volatile compound diversity is limited.[31] The formation of key flavor compounds such as pyrazines, pyridines, pyrroles, thiazoles, and Strecker aldehydes may require sufficient exogenous amino acids to participate in subsequent thermal reactions of the intermediates.[15,31] To further elucidate the effects of different amino acids, those types with varying isoelectric points and side chain groups were selected to combine with TTCA for thermal reactions. The browning intensity was significantly higher ($p < 0.05$) in the systems with added amino acids than in the TTCA control (Fig. 1c), likely because amino acids react with carbonyl compounds in later stages to form colored polymers.[32]

Volatile analysis revealed that all systems predominantly generated sulfur-containing compounds (Table 1 and Fig. 1d, e), which was driven by the high reactivity of H_2S and NH_3 released from TTCA degradation (Fig. 1f).[10] Results showed that the side chains of the added amino acids had a negligible influence on sulfur-containing flavor formation (Table 1). High levels of 2-methyl-3-furanthiol and 2-furfuryl thiol were detected across all systems. This consistent presence indicated that added amino acids did not inhibit the key pathway leading to these furans—namely, the dehydration and cyclization of deoxyosones during TTCA degradation (Fig. 1f).[33] Furthermore, sulfur heterocycles requiring the participation of α-dicarbonyls (*e.g.*, 2-methyl-thiophene, thieno[3,2-*b*]thiophene, and thiazole)

Table 1 Characteristic flavor compounds (μg L^{-1}) derived from the reactions between different amino acids and TTCA[a]

				Neutral				Acidic		Basic	
Compounds	RI[b]	RI[c]	Control	Cys	Gly	Ala	Met	Glu	Asp	His	Lys
Sufur-containing compounds											
Thiols and sulfides											
Dimethyl disulfide	1085	1037	ND	ND	ND	ND	0.956 ± 0.013a	ND	ND	ND	ND
3-Mercapto-2-butanone*	1273	1283	1.798 ± 0.025a	ND	ND	ND	ND	ND	ND	ND	ND
2-Methyl-3-furanthiol*	1302	1305	1.388 ± 0.207f	4.083 ± 0.092d	11.569 ± 0.165b	0.329 ± 0.008g	—	7.327 ± 0.222c	0.344 ± 0.007g	2.536 ± 0.149e	18.752 ± 1.061a
3-Mercapto-2-pentanone*	1352	1343	1.298 ± 0.021a	0.438 ± 0.01b	ND	ND	ND	ND	ND	ND	ND
Dimethyl trisulfide	1392	1370	ND	ND	ND	ND	2.031 ± 0.028a	ND	ND	ND	ND
2-Furfurylthiol*	1426	1402	4.107 ± 0.152d	11.591 ± 0.26c	15.254 ± 0.217b	2.133 ± 0.003e	ND	12.107 ±0.366c	3.176 ± 0.061d	0.38 ± 0.022f	29.295 ± 1.658a
3-Thiophenethiol*	1564	1530	0.178 ± 0.011e	12.892 ± 0.289a	0.74 ± 0.011c	ND	ND	0.405 ± 0.012e	ND	ND	2.31 ± 0.131b
2-Thiophenemethanethiol*	1702	1713	0.196 ± 0.012d	0.483 ± 0.011a	0.267 ± 0.004c	ND	ND	0.207 ± 0.006d	ND	ND	0.41 ± 0.023b
2-Methyl-3-[(2-methyl-3-thienyl)dithio]furan	1732	—	0.098 ± 0.006d	ND	2.804 ± 0.04b	ND	ND	0.574 ± 0.017c	ND	ND	4.428 ± 0.251a
1,2,3-Trithiolane	1794	—	0.378 ± 0.026a	ND	ND	ND	ND	ND	ND	ND	ND
3,3′-Dithiobis[2-methyl-furan]	2139	—	ND	ND	ND	ND	ND	3.946 ± 0.119b	ND	ND	6.862 ± 0.388a
Furfuryl sulfide	2274	2223	ND	ND	0.159 ± 0.002a	ND	ND	ND	0.025 ± 0b	ND	ND
Bis(2-furfuryl)sulfide	2419	—	0.042 ± 0.008b	0.972 ± 0.022a	—	ND	ND	ND	ND	ND	ND
Subtotal			9.483 ± 0.199d	30.46 ± 0.684b	30.794 ± 0.438b	2.461 ± 0.011f	2.987 ± 0.042ef	24.566 ± 0.743c	3.545 ± 0.068e	2.916 ± 0.171ef	62.057 ±3.512a
Kinds			9	6	6	2	2	6	4	2	5
Thiophenes											
Thiophene*	1016	1022	ND	ND	ND	ND	ND	ND	ND	ND	ND
3-Methyl-thiophene	1119	1106	ND	ND	10.192 ± 0.145a	ND	ND	ND	ND	ND	0.083 ± 0.005b
2,3-Dihydro-5-methyl-thiophene	1129	1156	0 ± 0e	0.058 ± 0.001d	0.167 ± 0.002b	ND	ND	0.126 ± 0.004c	ND	ND	0.204 ± 0.012a
2-Methyl-thiophene*	1135	1095	1.128 ± 0.159c	0.237 ± 0.005d	0.147 ± 0.002d	0.098 ± 0.002d	ND	5.389 ± 0.163b	0.141 ± 0.003d	0.48 ± 0.028d	12.21 ± 0.691a
2-Ethyl-thiophene	1179	1167	ND	ND	ND	ND	ND	0.062 ± 0.002c	ND	ND	0.083 ± 0.005b
2,5-Dimethyl-thiophene	1216	1202	ND	ND	0.464 ± 0.007b	0.76 ± 0.019a	ND	ND	ND	ND	0.461 ± 0.026b
2,3-Dimethyl-thiophene	1232	1212	ND	ND	0.038 ± 0.001b	ND	ND	0.207 ± 0.006a	ND	ND	ND
Dihydro-2-methyl-3(2*H*)-thiophenone	1511	1506	ND	ND	1.167 ± 0.017b	ND	ND	ND	ND	ND	1.77 ± 0.1a
2-Thiophenecarboxaldehyde*	1674	1679	2.196 ± 0.076b	1.06 ± 0.024c	0.541 ± 0.008e	ND	3.109 ± 0.043a	ND	0.125 ± 0.002f	0.078 ± 0.005f	0.695 ± 0.039d
5-Methyl-2-thiophenecarboxaldehyde*	1701	1785	3.649 ± 0.075a	2.535 ± 0.057c	ND	ND	ND	ND	ND	ND	2.808 ± 0.159b
2-Acetyl-3-methylthiophene	1754	1760	ND	ND	0.488 ± 0.007a	ND	ND	ND	ND	ND	0.388 ± 0.022b
Thieno[3,2-*b*]thiophene	1868	1843	1.302 ± 0.099b	7.967 ± 0.179a	0.659 ± 0.009d	0.038 ± 0.001f	0.063 ± 0.001f	0.39 ± 0.012e	0.192 ± 0.004f	0.105 ± 0.006f	0.964 ± 0.055c
1-(2-Thienyl)-1-propanone	1872	—	ND	ND	0.46 ± 0.007b	ND	ND	ND	ND	ND	0.584 ± 0.033a
2,5-Thiophenedicarboxaldehyde*	1911	—	0.724 ± 0.055d	1.261 ± 0.028a	1.015 ± 0.014c	ND	1.079 ± 0.015b	0.292 ± 0.009e	ND	ND	ND
2-Methylthieno[2,3-*b*] thiophene	1947	—	0.19 ± 0.023c	1.886 ± 0.042a	ND	ND	0.012 ± 0.000d	ND	ND	ND	0.24 ± 0.014b

Table 1 (*Contd.*)

Compounds	RI[b]	RI[c]	Control	Neutral				Acidic		Basic	
				Cys	Gly	Ala	Met	Glu	Asp	His	Lys
Subtotal			9.189 ± 0.392c	15.003 ± 0.337b	15.338 ± 0.218b	0.895 ± 0.022f	4.263 ± 0.059e	6.466 ± 0.196d	0.457 ± 0.009f	0.663 ± 0.039f	20.49 ± 1.16a
Kinds			6	7	13	3	4	7	3	3	14
Thiazoles											
Thiazole*	1240	1262	1.796 ± 0.128a	0.461 ± 0.01d	0.556 ± 0.008 cd	0.131 ± 0.003f	—	0.58 ± 0.018c	0.353 ± 0.007e	0.772 ± 0.045b	0.506 ± 0.029 cd
2-Methyl-thiazole*	1272	1278	0.194 ± 0.017d	0.579 ± 0.013b	ND	ND	ND	0 ± 0e	ND	0.612 ± 0.036a	0.277 ± 0.016c
2,5-Dimethyl-thiazole*	1301	1326	2.203 ± 0.143a	0.127 ± 0.003b	ND	ND	ND	0.188 ± 0.006b	ND	ND	ND
2-Ethyl-thiazole*	1319	1304	0.273 ± 0.008a	0.152 ± 0.003b	ND	ND	ND	0 ± 0c	ND	ND	ND
2,4,5-Trimethyl-thiazole*	1373	1390	3.199 ± 0.127a	0.928 ± 0.021b	0.38 ± 0.005c	ND	ND	0.442 ± 0.013c	ND	ND	0.209 ± 0.012d
4,5-Dimethyl-thiazole*	1378	1843	ND	ND	ND	ND	ND	ND	ND	ND	ND
5-Ethyl-2,4-dimethyl-thiazole*	1437	—	0.587 ± 0.014a	0.174 ± 0.004d	0.339 ± 0.005c	ND	ND	ND	ND	ND	0.38 ± 0.022b
2-Ethyl-4-methylthiazole*	1449	1410	1.278 ± 0.117a	0.284 ± 0.006b	0.219 ± 0.003b	0.014 ± 0.000c	ND	ND	0.018 ± 0c	ND	ND
2-Acetylthiazole	1646	1643	8.795 ± 0.213a	0.538 ± 0.012c	ND	ND	2.837 ± 0.04b	ND	ND	ND	ND
Subtotal			18.325 ± 0.744a	3.255 ± 0.073b	1.494 ± 0.021c	0.145 ± 0.004d	2.837 ± 0.04b	1.211 ± 0.037c	0.371 ± 0.007d	1.385 ± 0.081c	1.371 ± 0.078c
Kinds			8	9	4	2	1	3	2	2	4
Total contents of sufur-containing compounds			36.997 ± 1.1c	48.718 ± 1.094b	47.626 ± 0.678b	3.501 ± 0.037g	10.087 ± 0.14e	32.243 ± 0.975d	4.374 ± 0.084f	4.963 ± 0.291f	83.918 ± 4.749a
Total kinds of sufur-containing compounds			23	22	23	6	6	16	9	7	23
Nitrogen-containing heterocycles											
Pyridine	1189	1202	ND	ND	ND	ND	ND	ND	ND	ND	0.033 ± 0.002a
Methylpyrazine*	1214	1263	ND	0.343 ± 0.008d	1.623 ± 0.023b	ND	0.423 ± 0.006d	1.512 ± 0.046b	ND	0.692 ± 0.041c	4.055 ± 0.229a
2-Pyridinecarboxaldehyde	1186	—	ND	ND	ND	ND	ND	ND	ND	ND	1.239 ± 0.07a
Pyrazine*	1216	1209	ND	0.063 ± 0.001 cd	0.208 ± 0.003 cd	0.039 ± 0.001d	0.12 ± 0.002 cd	0.119 ± 0.004 cd	0.294 ± 0.006bc	0.498 ± 0.029b	5.699 ± 0.323a
3-Methyl-pyridine*	1307	1346	ND	0.076 ± 0.002a	ND	ND	ND	ND	ND	ND	ND
2,5-Dimethyl-pyrazine*	1320	1328	ND	0.679 ± 0.015b	0.423 ± 0.006c	ND	0.069 ± 0.001e	0.402 ± 0.012c	ND	0.129 ± 0.008d	0.927 ± 0.052a
2-(*n*-Propyl)-pyrazine	1476	1428	ND	ND	ND	ND	ND	ND	ND	ND	0.378 ± 0.021a
Pyrrole	1499	1518	ND	ND	0.228 ± 0.003a	ND	ND	0.12 ± 0.004b	ND	ND	ND
2-Methyl-1*H*-pyrrole	1534	1551	ND	ND	0.371 ± 0.005b	0.036 ± 0.001d	ND	0.139 ± 0.004c	ND	ND	0.411 ± 0.023a
1*H*-Pyrrole-2-carboxaldehyde	2002	2028	ND	ND	ND	ND	0.836 ± 0.012a	ND	ND	ND	ND
Subtotal			ND	1.161 ± 0.026d	2.853 ± 0.041b	0.076 ± 0.002e	1.448 ± 0.02d	2.292 ± 0.069c	0.294 ± 0.006e	1.319 ± 0.077d	12.741 ± 0.721a
Kinds			0	4	5	2	2	5	1	3	7
Oxygen-containing heterocycles											
Furan*	797	798	0.138 ± 0.01a	ND	ND	ND	ND	0 ± 0b	0 ± 0b	ND	ND
2-Methyl-furan*	851	829	0.019 ± 0.005f	ND	6.884 ± 0.098b	0.505 ± 0.012e	ND	4.741 ± 0.143c	0.276 ± 0.005ef	1.589 ± 0.093d	8.225 ± 0.465a
2-Ethyl-furan	913	949	ND	ND	0.041 ± 0.001b	ND	ND	0.042 ± 0.001b	0 ± 0c	ND	0.089 ± 0.005a
Furfural*	1457	1460	5.793 ± 0.155a	ND	1.05 ± 0.015e	0.242 ± 0.006g	1.968 ± 0.027c	1.019 ± 0.031e	3.589 ± 0.069b	1.369 ± 0.08d	0.664 ± 0.038f
2-Acetylfuran	1491	1500	ND	ND	ND	ND	ND	1.189 ± 0.036a	0.378 ± 0.007b	ND	ND
1-(2-Furanyl)-ethanone*	1497	1501	0.136 ± 0.077a	ND	ND	ND	ND	ND	ND	ND	ND

Table 1 (*Contd.*)

Compounds	RI[b]	RI[c]	Control	Neutral			Acidic			Basic		
				Cys	Gly	Ala	Met	Glu	Asp	His	Lys	
5-Methylfurfural	1542	1567	ND	ND	1.34 ± 0.019a	0.703 ± 0.017b	ND	ND	ND	ND	ND	
2(5*H*)-Furanone*	1748	1767	0.072 ± 0.005a	ND	ND	ND	ND	ND	ND	ND	ND	
4-Hydroxy-5-methyl-3(2*H*)-furanone*	2108	2124	ND	ND	ND	ND	ND	0.19 ± 0.006a	ND	ND	ND	
Subtotal			6.158 ± 0.231c	ND	9.314 ± 0.133a	1.45 ± 0.036g	1.968 ± 0.027f	7.182 ± 0.217b	4.243 ± 0.082d	2.958 ± 0.174e	8.978 ± 0.508a	
Kinds			5	0	4	3	1.000	5	3	2	3	
Total			43.155 ± 1.223d	49.878 ± 1.12c	59.793 ± 0.851b	5.027 ± 0.075f	13.503 ± 0.188e	41.717 ± 1.262d	8.911 ± 0.172e	9.24 ± 0.542e	105.637 ± 5.978a	
Total kinds			28	26	32	11	9	26	13	12	33	

[a] Notes: Results are presented as mean ± standard deviation; data within a row with different letters are significantly different ($p < 0.05$), as indicated by Duncan's multiple comparison tests ($n = 3$). [b] Linear retention indices calculated using a series of *n*-alkanes on a DB-WAX column (30 m × 0.25 mm × 0.25 μm). [c] Linear retention indices searched from https://www.flavornet.org and https://webbook.nist.gov/chemistry/. "ND": not detected. Compounds marked with an asterisk (*) were quantified using the standard curve method with internal standard calibration.

were detected, and were common to all systems supplemented with Gly, Lys, or Glu (Fig. 1f).[34] This reinforces that the core pathway for sulfur-containing flavor generation is governed by α-dicarbonyl formation rather than by the specific side chains of the added amino acids. The addition of the three exogenous amino acids can promote the retro-aldol cleavage of deoxyosones, yielding more short-chain α-dicarbonyl compounds and reductive ketones, which expanded flavor diversity (including sulfur compounds and pyrazines) and contributed to enhanced browning.[13] Gly supplementation produced the greatest variety of flavor compounds, possibly due to its propensity to form short-chain reactive aldehydes.[35] Lys significantly increased flavor variety ($p < 0.05$), likely because its additional amino group boosted α-dicarbonyl formation *via* reactions with sugar chains.[36]

Compared to the TTCA control, systems with Gly, Lys, or Glu showed a reduced thiazole content/variety but increased nitrogenous heterocycles, confirming greater NH_3 participation in pyrazine formation (Fig. 1f).[37] The TTCA-Lys thermal reaction system could generate pyrazines. At the system pH (7.0), some Lys residues remained undissociated and acted as nucleophiles, reacting with sugar residues to produce short-chain α-dicarbonyls that subsequently formed pyrazines[38] (Fig. 1f). In contrast, TTCA-His produced less meat or roasting aroma (Table 1), as its imino group is less reactive than amino group to form carbonyl compounds as a nucleophile.[29] Moreover, the imidazole group with strong basic properties has a lower reactivity, and is less likely to participate in the formation of flavor compounds.[35] In addition to Lys, the TTCA thermal reaction system supplemented with Glu detected a considerable amount of pyrazine compounds, which is consistent with previous research.[39] Beyond pyrazines, pyrroles were detected in all three systems, linked to reactions between α-dicarbonyls (MGO/GO) and NH_3 (Fig. 1f).[40] Among them, 2-methylpyrrole and pyrrole were synthesized *via* an aldol condensation reaction between MGO/GO and acetaldehyde, followed by nucleophilic addition with NH_3 and dehydration. 2-Pyrrolecarboxaldehyde was produced by nucleophilic addition of NH_3 to a 3-DX isomer, followed by dehydration and cyclization (Fig. 1f).[41] The large amount of pyridine compounds in the TTCA-Lys reaction system was generated by the Strecker degradation reaction between Lys and α-dicarbonyl compounds, followed by subsequent dehydration reactions (Fig. 1f).[42]

Furans (mainly 2-methylfuran and furfural) were formed in TTCA reaction systems with Gly, Lys, or Glu but not in a TTCA-Cys system, indirectly confirming the critical role of H_2S from Cys degradation in diverting precursors toward sulfur-containing flavors. In summary, supplementing TTCA with Gly or Lys enriched the overall flavor profile (sulfur compounds and pyrazines), while Glu specifically promoted pyrazine formation ($p < 0.05$). Exogenous amino acids help shift the reaction equilibrium by ensuring sufficient α-dicarbonyl precursors for key flavor pathways.[43] Simultaneously, incorporating various exogenous amino acids can markedly enhance the browning development in the TTCA thermal reaction system. These results suggest that combining Gly, Lys, or Glu

with TTCA could enhance TTCA's versatility for generating desired colors and flavors in diverse food applications.

3.3 Extremely high environmental stability of TTCA and ARP intermediates to act as natural flavoring additives

The storage environment is a key factor affecting the structure, content and physicochemical properties of all kinds of chemical products in the storage process.[44] In this study, the storage stability of TTCA and ARP was investigated. The key finding is that TTCA exhibits superior storage stability compared to ARPs across all conditions tested, attributed to its stable cyclic molecular structure.[3] Both intermediates were highly stable at 4 °C and 25 °C. Degradation became noticeable only under stress conditions: at 40 °C, and the TTCA concentration decreased by 7.06% after 60 days, less than ARP's 12.17% loss. The increased degradation at elevated temperatures is linked to water autoionization,[45] which catalyzes the enolization and ring-opening of ARPs.[44] Corresponding increases in the A_{294} and A_{420} values at 40 °C (Fig. 2c and d) indicate the formation of carbonyl intermediates and browning products.[21]

The stability of TTCA and ARP solutions stored at pH 5.5, 7 and 9 was monitored for 60 days at room temperature (Fig. 2e–h). The intermediates maintained stable concentrations under acidic and neutral conditions (pH 5.5 and 7). In contrast, at pH 9, the concentrations of TTCA and ARPs decreased by 11.19% and 21.25% after 60 days, respectively. Meanwhile, the rise of A_{294} and A_{420} also indicate the alkaline-promoted degradation into downstream products. The slight decrease in TTCA concentration at pH 5.5—accompanied by opposing trends in A_{420} (increase) and A_{294} (decrease)—suggested a transformation distinct from degradation, potentially due to acid-catalyzed hydrolysis or reversion to *N*-xylosylamine.[45] This phenomenon is attributed to the formation of rearrangement reaction by the deprotonation of imine positive ions, so the presence of H^+ under acidic conditions could promote the reverse reaction.[21]

The moisture content and water activity values of food products are key indicators of their shelf life and eating quality.[46] The stability of solid TTCA and ARP was assessed for 60 days under varying humidity levels. When stored under dry conditions (a_w 0.113) for 60 days, the TTCA content decreased by only 13.5% (Fig. 2i). This exceptional stability implies lower storage losses, reduced packaging demands, and potentially extended shelf-life in food applications. Elevated moisture activity significantly accelerated the degradation and browning of both TTCA and ARP. Colorimetric analysis (L^*, a^*, b^*, ΔE) showed that increased a_w led to darker samples (decreased L^*) and more pronounced overall color change (ΔE) (Table 2). Notably, the ΔE values for ARP were consistently higher than those for TTCA under all humidity conditions, further corroborating TTCA's superior stability. A semi-quantitative estimate indicates that TTCA's degradation rate in high humidity (a_w 0.843) is approximately 60% slower than that of ARP (Fig. 2j).

In summary, TTCA possesses significantly greater environmental stability than ARP. Optimal storage conditions are low temperature, acidic-to-neutral pH, and low humidity, while high temperature, alkaline pH, and high moisture accelerate

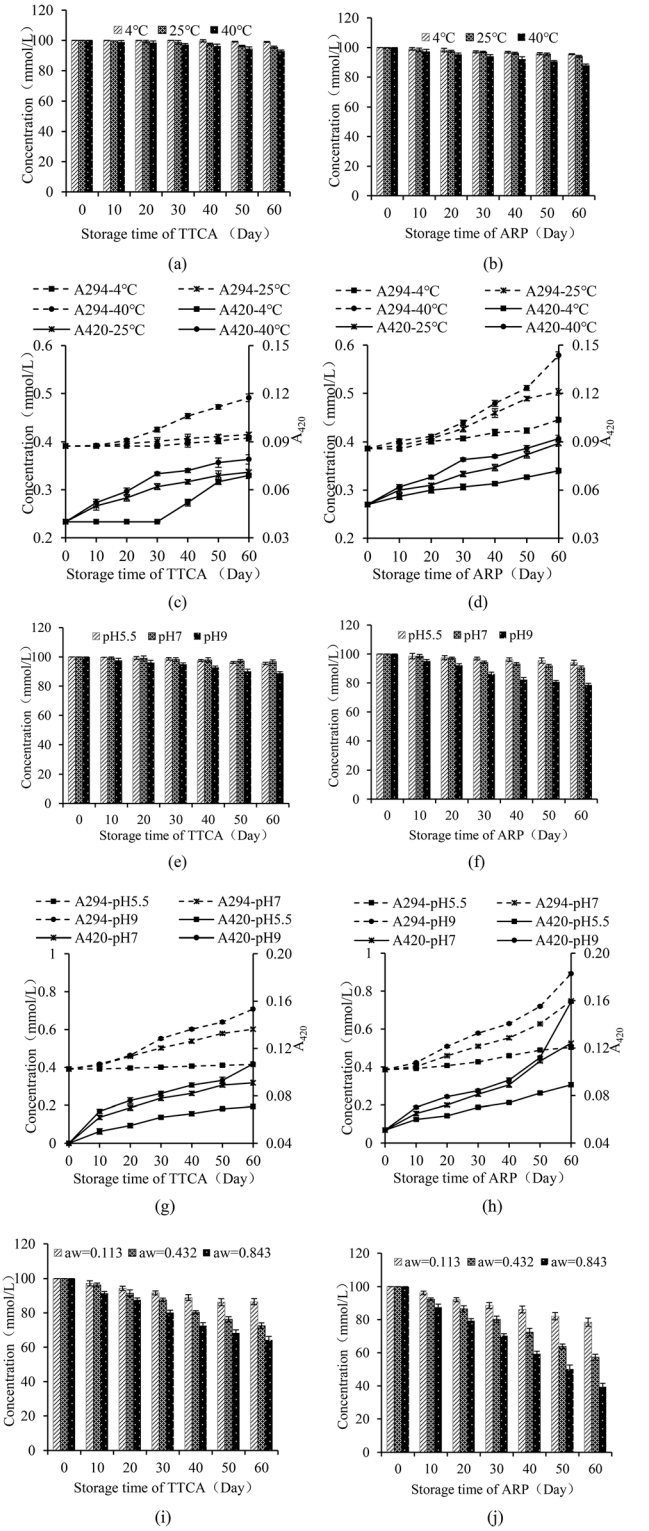

Fig. 2 Residual content of TTCA (a) and ARPs (b) in solutions at different temperatures; absorbance at 420 nm and 294 nm for TTCA (c) and ARP (d) solutions at different temperatures; residual content of TTCA (e) and ARPs (f) in solutions at different pH levels; absorbance at 420 nm and 294 nm for TTCA (g) and ARP (h) solutions at different pH levels; and residual content of solid TTCA (i) and ARPs (j) after 60 days at different water activities.

Table 2 Variations in TTCA (a) and ARP (b) contents in solid samples over 60 days of storage at different water activities

		a_w			
MRI	Indicator	Control	0.113	0.432	0.843
TTCA	L^*	88.39 ± 0.03a	81.36 ± 0.02b	77.39 ± 0.04c	72.34 ± 0.02d
	a^*	5.19 ± 0.01d	7.71 ± 0.03c	9.19 ± 0.02b	11.63 ± 0.04a
	b^*	11.13 ± 0.02d	16.78 ± 0.04c	22.36 ± 0.03b	27.63 ± 0.01a
	ΔE	—	9.36c	16.22b	23.90a
ARP	L^*	87.68 ± 0.03a	79.36 ± 0.03b	62.18 ± 0.03c	51.03 ± 0.03d
	a^*	6.21 ± 0.03d	11.39 ± 0.03c	17.68 ± 0.03b	21.39 ± 0.03a
	b^*	13.19 ± 0.03d	20.38 ± 0.03c	29.63 ± 0.03b	37.68 ± 0.03a
	ΔE	—	12.16c	32.44b	46.62a

degradation. These results confirm TTCA's extended effective shelf life and underscore the necessity for cool, dry, and sealed storage for practical applications as a stable flavor precursor.

3.4 Antioxidant properties of MRIs demonstrate promising potential as alternatives to synthetic antioxidants

The antioxidant capacities of TTCA and ARP intermediates and complete Maillard reaction products (MRPs) were evaluated in this study. The chelating ability of Fe^{2+} helps to reduce the occurrence of lipid oxidation, and is an important indicator for evaluating antioxidants.[7] A concentration-dependent Fe^{2+} chelating ability was observed for TTCA and ARPs (Fig. 3a). Fe^{2+} can coordinate with the carbonyl oxygen atom on the xylose segment of Amadori compounds, forming a five-membered chelating ring.[7] Compared to the ARP molecule, the TTCA compound can provide stronger overall molecular polarity and more polar sites (including hydroxyl and carbonyl groups) in its possible tautomeric forms (Table S1).[36] This enhanced polar characteristic allowed the TTCA molecule to interact more effectively with solvent water molecules in aqueous solutions through electrostatic interactions and dynamic hydrogen-bonding networks, thereby forming more stable solvated complexes.[47] Therefore, TTCA compound molecules have more sites that can form complexes with Fe^{2+}, and the complexes formed may be more stable than those formed by ARP, which likely directly leads to a higher Fe^{2+} chelating ability of TTCA (71.35%) than that of the ARP (51.03%) (Fig. 3a). Besides, MRPs always revealed a higher Fe^{2+} chelating ability than that of TTCA and ARP compounds. Some melanoidins in MRPs can be natural free radical scavengers in the food system.

The reducing power, reflecting a substance's electron transfer ability, was measured to further evaluate the antioxidant activity.[7] A positive correlation was observed between the concentration of MRIs (0.5–3 mg mL^{-1}) and their reducing power (Fig. 3b). This can be attributed to reductive ketones and hydroxyl-containing compounds in the intermediates, which can donate electrons or hydrogen atoms to reduce the ferricyanide complex.[23] Notably, ARPs exhibited stronger reducing properties than TTCA. This difference likely stems from the role of free thiol groups in ARPs, which possess strong electron-donating ability due to their S–H bonds. In contrast, the thiol groups in TTCA are involved in forming a stable five-membered ring, leaving no exposed free thiols available for reduction.[48] Furthermore, MRPs exhibited a stronger reducing power than that of their intermediates at all tested concentrations, with a rapid increase as the concentration increased, which is consistent with the existing research results.[47]

The chelating action on transition metals and the reducing action can inhibit lipid oxidation. Within the concentrations of 0.5 to 2.5 mg mL^{-1}, ARP/TTCA inhibited lipid peroxidation more than the MRPs, indicating ARP's better efficacy (Fig. 3c). As the concentration increased to 3.0 mg mL^{-1}, the inhibition rate for lipid peroxidation of MRPs increased from 2.18% to 36.39%, exceeding that of ARP (29.18%) and TTCA (31.30%) at 3.0 mg mL^{-1} (Fig. 3c). The increased concentration of TTCA or ARP beyond a certain point did not lead to a corresponding significant improvement in the inhibition of lipid peroxidation. This observed plateau in efficacy could result from several factors, such as potential solubility limitations of TTCA and ARPs compared to MRPs (rich in aldehydes and ketones) in the emulsion system,[27,30] or the attainment of a saturation point for their antioxidant action under these specific conditions. The results confirmed that TTCA or ARPs could be one reason for the antioxidant activity of the Maillard reaction during food processing and storage. However, at higher concentrations, the MRPs demonstrated superior performance compared to their precursors, suggesting that they possess better emulsion system compatibility and contain a greater number of compounds with strong antioxidant activity.

The DPPH free radical scavenging ability typically reflects the hydrogen-donating ability of antioxidants.[49] The scavenging rates of TTCA and ARP increased with their concentration during the range of 0.5 to 3.0 mg mL^{-1} (Fig. 4a). Their effect was weaker than that of MRPs and considerably lower than that of ascorbic acid, which achieved nearly 100% scavenging across the same range. Similar concentration-dependent trends were observed for superoxide anion and hydroxyl radical scavenging (Fig. 4a and b). At a concentration of 3.0 mg mL^{-1}, the superoxide anion radical scavenging activities of TTCA and ARP are functionally comparable to that of 0.5 mg mL^{-1} ascorbic acid, suggesting that approximately 6 g of TTCA could theoretically replace 1 g of ascorbic acid in antioxidant applications. MRPs consistently demonstrated a stronger radical scavenging ability than that of the intermediates, with activity rising sharply at higher concentrations (Fig. 4a–c), consistent with prior reports.[47] This enhanced activity is attributed to the complex mixture of cross-linked polymers, aldehydes, ketones, and

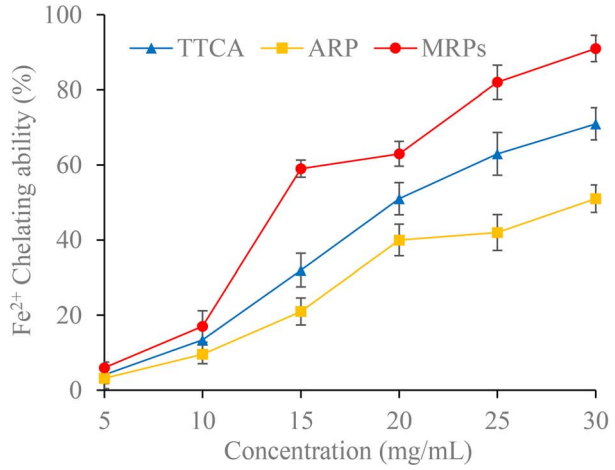

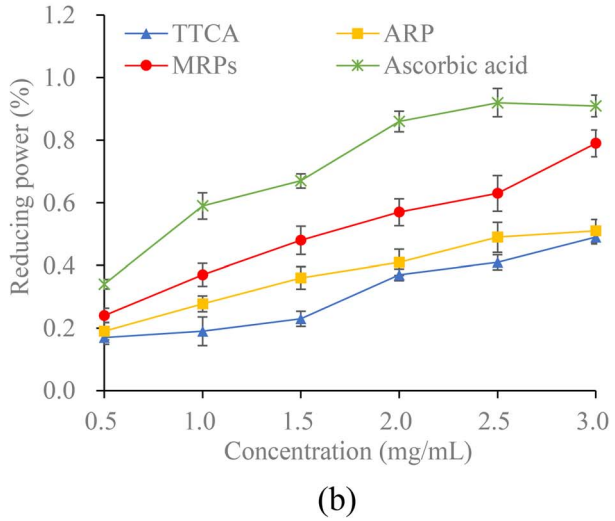

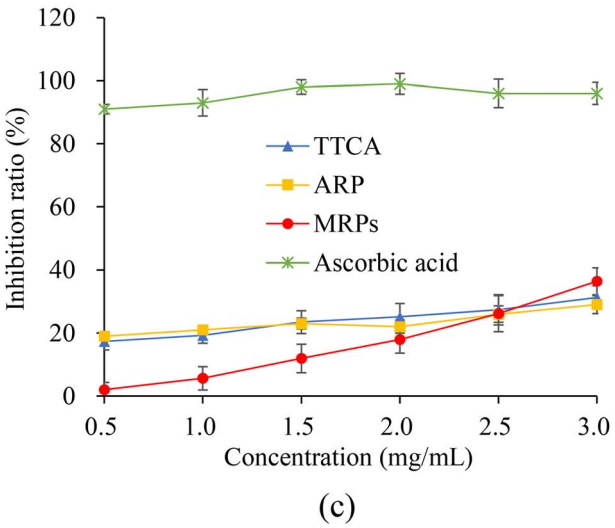

Fig. 3 Fe^{2+} chelating activity (a) and reducing power (b) of TTCA, ARPs and MRPs and inhibition of TTCA, ARPs, MRPs and ascorbic acid on lipid peroxidation induced by iron (c).

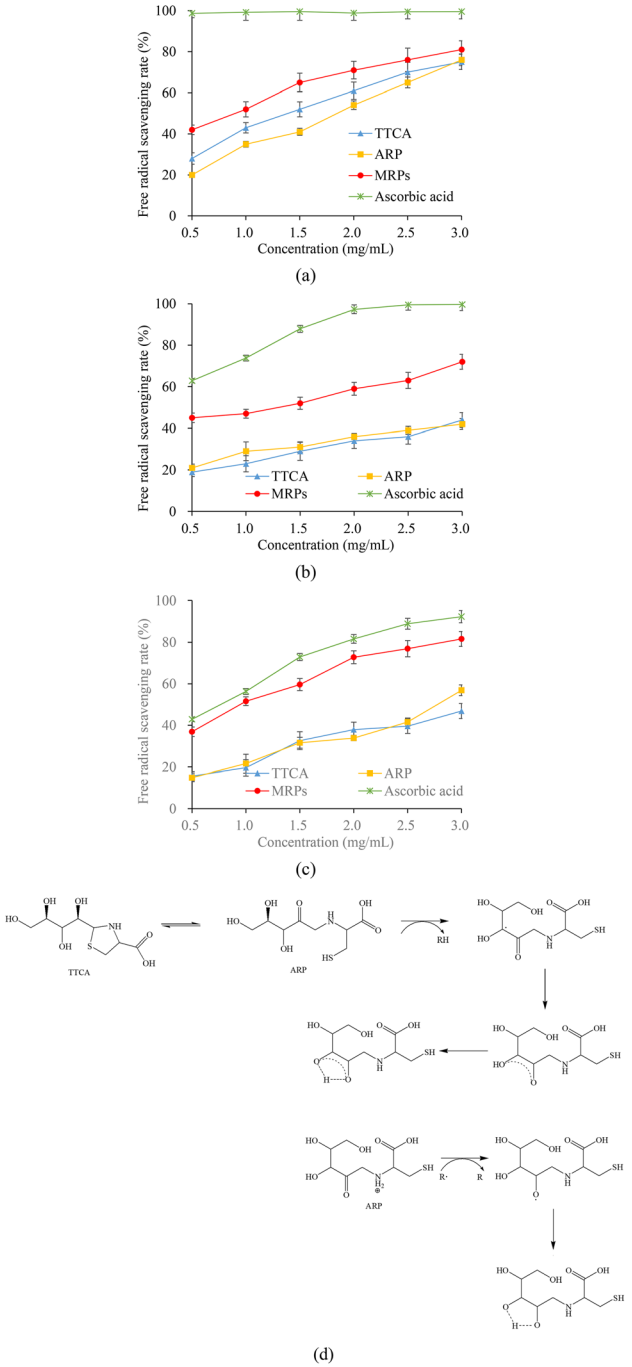

Fig. 4 DPPH radical scavenging activity (a), hydroxyl radical scavenging activity (b) and superoxide anion radical scavenging activity (c) of TTCA, ARPs, MRPs and ascorbic acid and possible pathway of the reaction between free radicals and ARPs (R• is the free radical) (d).

heterocyclic compounds formed in the later Maillard stages, which exert antioxidant effects through multiple pathways.[27] In summary, while MRIs such as TTCA and ARP contribute to controlled flavor formation, the final MRPs exhibit superior antioxidant properties. Therefore, a combination of MRIs and MRPs holds potential as dual-function ingredients, serving as both natural flavor enhancers and antioxidants in food systems.

TTCA and ARP compounds, derived from xylose and cysteine, exhibit antioxidant properties distinct from a simple cysteine–xylose mixture, indicating that structural differences at the molecular level are responsible,[50] while free sugars like pentoses, hexoses, and ketoses predominantly exist in a closed-ring form in solutions, with minimal reactive open-chain carbonyls.[51] For MRIs, the conjugated electron cloud structure between the enol and aminium ions leads to an equilibrium of isomeric interconversion between their open-ring and closed-ring forms, with the open-chain conformation becoming a significant configuration in aqueous media.[52] This provides abundant free carbonyl groups capable of donating electrons to neutralize free radicals.[7] Based on this, a possible pathway for the intermediates to scavenge free radicals is proposed (Fig. 4d). TTCA and ARPs can donate hydrogen atoms to free radicals, stabilizing them and terminating chain reactions. The radical electron can localize on the carbon adjacent to the carbonyl group on the xylose residue, where resonance and intramolecular hydrogen bonding lead to a thermodynamically stable intermediate. Alternatively, the carbonyl group itself may be attacked, with the radical electron transferring to the oxygen atom, followed by stabilization *via* intramolecular hydrogen bonding.[7,53,54] Research also found that the free radical scavenging ability of ARPs is consistent with its electron-donating or hydrogen-donating properties and specifically proposed that its metal chelating ability may also be related to this principle.[39] Although this study indicates that TTCA and ARPs exhibited certain antioxidant activity, its long-term stability in complex food systems and the production costs at scale still require further evaluation. Therefore, MRIs can serve as natural flavor precursors to achieve controlled formation of processing flavors and provide partial antioxidant functions, suggesting a potential practical value.

4 Conclusion

This study demonstrates that the Xyl-Cys MRIs including TTCA and ARPs could act as dual-functional, sustainable platforms, integrating efficient flavor precursor properties with certain natural antioxidant activities. The flavor profile released from TTCA can be regulated from "meaty" to "roasted nutty" notes through simply modulating thermal processing parameters (pH and temperature). The addition of exogenous amino acids can further enrich the diversity of roasted flavor compounds such as pyrazines. This significantly enhances the processing adaptability of the flavor precursors of MRIs. Compared to MRPs, TTCA or the ARP exhibits superior stability for commercial applications, which can retain over 90% of its content after 60 days of storage under ambient, neutral, and dry conditions. This stability ensures consistent performance and reliability during the storage, transportation, and use of TTCA or ARP as an ingredient, significantly reducing the risks of raw material loss and flavor variability due to degradation. TTCA and ARP compounds revealed increased Fe^{2+} chelating ability, reducing power, and free radical scavenging ability with the increase in concentration, demonstrating certain antioxidant capabilities. By combining flavor enhancement with moderate oxidative stability contributed by MRIs, this approach provides a new direction for "clean-label" food development that may enable a partial reduction in reliance on synthetic antioxidants and flavor additives. In summary, this work supports the potential of TTCA or the ARP to act as a sustainable platform for natural flavoring and supporting antioxidant properties. It offers a feasible strategy for improving the food quality and stability and aligns with the pursuit of greener food processing practices.

Author contributions

Di Kang and Songjin Zheng conceived the study and designed and supervised the research. Yun Zhai and Yuying Fu outlined the study, performed the literature search, and prepared the original draft and figures. Lin Jiang, Yuan Hu, Haifeng Wang and Teng Li assisted in preparing the figures and the draft. All the authors have read and approved the final version to be published.

Conflicts of interest

The authors declare no competing financial interest. This article does not contain any study with human participants or animals performed by any of the authors.

Data availability

All the data generated or analyzed during this study are included in the manuscript.

Supplementary information (SI): data on the structural confirmation of TTCA, the degradation and flavor formation patterns under various thermal processing conditions (temperature, pH), as well as the dynamic changes of the key precursor (Cys). These data serve as robust supporting material for the conclusions drawn in the main text regarding the antioxidant activity, stability, and flavor contribution of TTCA and ARP. See DOI: https://doi.org/10.1039/d5fb00932d.

Acknowledgements

The research was supported by the Zhejiang Provincial Natural Science Foundation of China under Grant No. LQN25C200010, the Scientific Research Fund of Zhejiang Provincial Education Department under Grant No. Y202353299, and the Fundamental Research Funds for the Provincial Universities of Zhejiang under Grant No. QRK23003.

References

1 R. Bel-Rhlid, R. G. Berger and I. Blank, Bio-mediated generation of food flavors – Towards sustainable flavor production inspired by nature, *Trends Food Sci. Technol.*, 2018, **78**, 134–143.
2 G. P. Rizzi, *Chemically Reducing Properties of Maillard Reaction Intermediates*, 2019, pp. 35–40.
3 D. S. Mottram, Flavour formation in meat and meat products: a review, *Food Chem.*, 1998, **62**, 415–424.
4 Y. Zhai, H. Cui, K. Hayat, S. Hussain, M. U. Tahir, J. Yu, C. Jia, X. Zhang and C.-T. Ho, Interaction of Added l-Cysteine with

2-Threityl-thiazolidine-4-carboxylic Acid Derived from the Xylose–Cysteine System Affecting Its Maillard Browning, *J. Agric. Food Chem.*, 2019, **67**, 8632–8640.

5 F. Shahidi, L. J. Rubin and L. A. D'Souza, Meat flavor volatiles: a review of the composition, techniques of analysis, and sensory evaluation, *Crit. Rev. Food Sci. Nutr.*, 1986, **24**, 141–243.

6 Amadori Compounds of Cysteine and Their Role in the Development of Meat Flavor, https://www.researchgate.net/publication/289728874_Amadori_Compounds_of_Cysteine_and_Their_Role_in_the_Development_of_Meat_Flavor, accessed 4 December 2025.

7 S. Benjakul, W. Visessanguan, V. Phongkanpai and M. Tanaka, Antioxidative activity of caramelisation products and their preventive effect on lipid oxidation in fish mince, *Food Chem.*, 2005, **90**, 231–239.

8 H. Cui, J. Yu, Y. Zhai, L. Feng, P. Chen, K. Hayat, Y. Xu, X. Zhang and C.-T. Ho, Formation and fate of Amadori rearrangement products in Maillard reaction, *Trends Food Sci. Technol.*, 2021, **115**, 391–408.

9 Y. Zhai, H. Cui, K. Hayat, S. Hussain, M. U. Tahir, S. Deng, Q. Zhang, X. Zhang and C.-T. Ho, Transformation between 2-Threityl-thiazolidine-4-carboxylic Acid and Xylose–Cysteine Amadori Rearrangement Product Regulated by pH Adjustment during High-Temperature Instantaneous Dehydration, *J. Agric. Food Chem.*, 2020, **68**, 10884–10892.

10 V. A. Yaylayan, Recent Advances in the Chemistry of Strecker Degradation and Amadori Rearrangement: Implications to Aroma and Color Formation, *Food Sci. Technol. Res.*, 2003, **9**, 1–6.

11 H. Zhang, H. Cui, X. Xia, S. Hussain, K. Hayat, X. Zhang and C.-T. Ho, Control Formation of Furans and Pyrazines Resulting from Dual Glycation Sites in Nα,Nε-Di(1-deoxy-d-xylulos-1-yl)lysine via Elevating Thermal Degradation Temperatures, *J. Agric. Food Chem.*, 2024, **72**, 25261–25274.

12 L. Feng, H. Cui, P. Chen, K. Hayat, X. Zhang and C.-T. Ho, Promoted Formation of Pyrazines and Sulfur-Containing Volatile Compounds through Interaction of Extra-Added Glutathione or Its Constituent Amino Acids and Secondary Products of Thermally Degraded N-(1-Deoxy-d-ribulos-1-yl)-Glutathione, *J. Agric. Food Chem.*, 2022, **70**, 9095–9105.

13 X. Xia, T. Zhou, H. Zhang, H. Cui, F. Zhang, K. Hayat, X. Zhang and C.-T. Ho, Simultaneously Enhanced Formation of Pyrazines and Furans during Thermal Degradation of the Glycyl-l-glutamine Amadori Compound by Selected Exogenous Amino Acids and Appropriate Elevated Temperatures, *J. Agric. Food Chem.*, 2023, **71**, 4346–4357.

14 Y. Zhai, H. Cui, Q. Zhang, K. Hayat, X. Wu, S. Deng, X. Zhang and C.-T. Ho, Degradation of 2-Threityl-Thiazolidine-4-Carboxylic Acid and Corresponding Browning Accelerated by Trapping Reaction between Extra-Added Xylose and Released Cysteine during Maillard Reaction, *J. Agric. Food Chem.*, 2021, **69**, 10648–10656.

15 Y. Zhai, H. Cui, K. Hayat, T. Li, X. Wu, Y. Fu, X. Zhang and C.-T. Ho, Regulated Formation of Inhibited Color and Enhanced Flavor Derived from Heated 2-Threityl-Thiazolidine-4-Carboxylic Acid with Additional Cysteine Targeting at Different Degradation Stages, *J. Agric. Food Chem.*, 2023, **71**, 14300–14311.

16 Y. Luo, S. Li and C.-T. Ho, Key Aspects of Amadori Rearrangement Products as Future Food Additives, *Molecules*, 2021, **26**, 4314.

17 B. Kebede, T. Grauwet, T. Andargie, G. Sempiri, S. Palmers, M. Hendrickx and A. Van Loey, Kinetics of Strecker aldehyde formation during thermal and high pressure high temperature processing of carrot puree, *Innovative Food Sci. Emerging Technol.*, 2017, **39**, 88–93.

18 C. Kanzler, H. Schestkowa, P. T. Haase and L. W. Kroh, Formation of Reactive Intermediates, Color, and Antioxidant Activity in the Maillard Reaction of Maltose in Comparison to d-Glucose, *J. Agric. Food Chem.*, 2017, **65**, 8957–8965.

19 W. Wang, Y. Bao and Y. Chen, Characteristics and antioxidant activity of water-soluble Maillard reaction products from interactions in a whey protein isolate and sugars system, *Food Chem.*, 2013, **139**, 355–361.

20 L. N. Vhangani and J. Van Wyk, Antioxidant activity of Maillard reaction products (MRPs) derived from fructose–lysine and ribose–lysine model systems, *Food Chem.*, 2013, **137**, 92–98.

21 J. Limsuwanmanee, M. Chaijan, S. Manurakchinakorn, W. Panpipat, S. Klomklao and S. Benjakul, Antioxidant activity of Maillard reaction products derived from stingray (Himantura signifier) non-protein nitrogenous fraction and sugar model systems, *LWT–Food Sci. Technol.*, 2014, **57**, 718–724.

22 M.-N. Maillard, C. Billaud, Y.-N. Chow, C. Ordonaud and J. Nicolas, Free radical scavenging, inhibition of polyphenoloxidase activity and copper chelating properties of model Maillard systems, *LWT–Food Sci. Technol.*, 2007, **40**, 1434–1444.

23 I. G. Hwang, H. Y. Kim, K. S. Woo, J. Lee and H. S. Jeong, Biological activities of Maillard reaction products (MRPs) in a sugar–amino acid model system, *Food Chem.*, 2011, **126**, 221–227.

24 G. M. Williams, M. J. Iatropoulos and J. Whysner, Safety Assessment of Butylated Hydroxyanisole and Butylated Hydroxytoluene as Antioxidant Food Additives, *Food Chem. Toxicol.*, 1999, **37**, 1027–1038.

25 W.-K. Jung, P.-J. Park, C.-B. Ahn and J.-Y. Je, Preparation and antioxidant potential of maillard reaction products from (MRPs) chitooligomer, *Food Chem.*, 2014, **145**, 173–178.

26 H. Cui, K. Hayat, C. Jia, E. Duhoranimana, Q. Huang, X. Zhang and C.-T. Ho, Synergistic Effect of a Thermal Reaction and Vacuum Dehydration on Improving Xylose–Phenylalanine Conversion to N-(1-Deoxy-d-xylulos-1-yl)-phenylalanine during an Aqueous Maillard Reaction, *J. Agric. Food Chem.*, 2018, **66**, 10077–10085.

27 F. Gu, J. M. Kim, K. Hayat, S. Xia, B. Feng and X. Zhang, Characteristics and antioxidant activity of ultrafiltrated Maillard reaction products from a casein–glucose model system, *Food Chem.*, 2009, **117**, 48–54.

28 S. Wu, X. Dai, F. Shilong, M. Zhu, X. Shen, K. Zhang and S. Li, Antimicrobial and antioxidant capacity of glucosamine-zinc(II) complex via non-enzymatic browning reaction, *Food Sci. Biotechnol.*, 2018, **27**, 1–7.

29 T. Kocadağlı and V. Gökmen, Investigation of α-Dicarbonyl Compounds in Baby Foods by High-Performance Liquid Chromatography Coupled with Electrospray Ionization Mass Spectrometry, *J. Agric. Food Chem.*, 2014, **62**, 7714–7720.

30 D. S. Mottram and J. S. Elmore, in *Controlling Maillard Pathways To Generate Flavors*, American Chemical Society, 2010, vol. 1042, pp. 143–155.

31 S. Deng, H. Cui, K. Hayat, Y. Zhai, Q. Zhang, X. Zhang and C.-T. Ho, Comparison of pyrazines formation in methionine/glucose and corresponding Amadori rearrangement product model, *Food Chem.*, 2022, **382**, 132500.

32 M. Friedman, Food Browning and Its Prevention: An Overview, *J. Agric. Food Chem.*, 1996, **44**, 631–653.

33 T. Zhou, M. Huang, H. Cui, P. Chen, K. Hayat, X. Zhang and C.-T. Ho, Exogenous Alanine Promoting the Reaction between Amadori Compound and Deoxyxylosone and Inhibiting the Formation of 2-Furfural during Thermal Treatment, *J. Agric. Food Chem.*, 2024, **72**, 5878–5886.

34 M. Liu, J. Yu, T. Zhou, H. Xu, K. Hayat, X. Zhang and C.-T. Ho, Formation Priority of Pyrazines and 2-Acetylthiazole Dependent on the Added Cysteine and Fragments of Deoxyosones during the Thermal Process of the Glycine–Ribose Amadori Compound, *J. Agric. Food Chem.*, 2022, **70**, 11643–11651.

35 H.-I. Hwang, T. G. Hartman and C.-T. Ho, Relative Reactivities of Amino Acids in Pyrazine Formation, *J. Agric. Food Chem.*, 1995, **43**, 179–184.

36 A.-N. Yu and A.-D. Zhang, The effect of pH on the formation of aroma compounds produced by heating a model system containing l-ascorbic acid with l-threonine/l-serine, *Food Chem.*, 2010, **119**, 214–219.

37 S. Deng, Y. Zhai, H. Cui, K. Hayat, X. Zhang and C.-T. Ho, Mechanism of Pyrazine Formation Intervened by Oxidized Methionines during Thermal Degradation of the Methionine–Glucose Amadori Compound, *J. Agric. Food Chem.*, 2022, **70**, 14457–14467.

38 T. Zhou, M. Huang, H. Cui, S. Hussain, K. Hayat, X. Zhang and C.-T. Ho, Disclosing the Nitrogen Sources via Isotope Labeling Technique and the Formation Mechanism of Pyrazine and Alkylpyrazines during the Heat Treatment of N-(1-Deoxy-d-xylulos-1-yl)-alanine and Exogenous Alanine, *J. Agric. Food Chem.*, 2024, **72**, 18630–18637.

39 H. Zhan, H. Cui, J. Yu, K. Hayat, X. Wu, X. Zhang and C.-T. Ho, Characteristic flavor formation of thermally processed N-(1-deoxy-α-d-ribulos-1-yl)-glycine: Decisive role of additional amino acids and promotional effect of glyoxal, *Food Chem.*, 2022, **371**, 131137.

40 A.-N. Yu and A.-D. Zhang, The effect of pH on the formation of aroma compounds produced by heating a model system containing l-ascorbic acid with l-threonine/l-serine, *Food Chem.*, 2010, **119**, 214–219.

41 X. Gao, Y. Duan, H. Song and P. Yang, Unraveling the mechanism of aroma formation in the maillard reaction of roasted Wuyi rock tea: Focus on furfural, tea pyrrole, and 1-ethyl-1H-Pyrrole, *Food Biosci.*, 2025, **71**, 107137.

42 R. Bel-Rhlid, R. G. Berger and I. Blank, Bio-mediated generation of food flavors – Towards sustainable flavor production inspired by nature, *Trends Food Sci. Technol.*, 2018, **78**, 134–143.

43 T. Zhou, M. Huang, H. Cui, P. Chen, K. Hayat, X. Zhang and C.-T. Ho, Exogenous Alanine Promoting the Reaction between Amadori Compound and Deoxyxylosone and Inhibiting the Formation of 2-Furfural during Thermal Treatment, *J. Agric. Food Chem.*, 2024, **72**, 5878–5886.

44 N. V. Harohally, S. M. Srinivas and S. Umesh, ZnCl2-mediated practical protocol for the synthesis of Amadori ketoses, *Food Chem.*, 2014, **158**, 340–344.

45 *Amino-carbonyl reactions in food and biological systems : proceedings of the 3rd International Sympo*, https://www.las.ac.cn/front/book/detail?id=7153bffee43b00b5bfe66b85b3efbe3a, accessed 4 December 2025.

46 X. Wang, C. Wei, D. Wei and C. Yang, Impact of Amadori rearrangement products of cysteine-xylose-glutamic acid on meat flavor development, *Food Res. Int.*, 2026, **230**, 118535.

47 D. A. Cortés Yáñez, M. Gagneten, G. E. Leiva and L. S. Malec, Antioxidant activity developed at the different stages of Maillard reaction with milk proteins, *LWT–Food Sci. Technol.*, 2018, **89**, 344–349.

48 C. Kanzler, P. T. Haase, H. Schestkowa and L. W. Kroh, Antioxidant Properties of Heterocyclic Intermediates of the Maillard Reaction and Structurally Related Compounds, *J. Agric. Food Chem.*, 2016, **64**, 7829–7837.

49 J. A. Rufián-Henares and F. J. Morales, Functional properties of melanoidins: In vitro antioxidant, antimicrobial and antihypertensive activities, *Food Res. Int.*, 2007, **40**, 995–1002.

50 B. Cämmerer, W. Jalyschko and L. W. Kroh, Intact carbohydrate structures as part of the melanoidin skeleton, *J. Agric. Food Chem.*, 2002, **50**, 2083–2087.

51 D. M. T. Nguyen, J. P. Bartley and W. O. S. Doherty, Combined Fenton Oxidation and Chemical Coagulation for the Treatment of Melanoidin/Phenolic Acid Mixtures and Sugar Juice, *Ind. Eng. Chem. Res.*, 2017, **56**, 1385–1393.

52 H. Cui, C. Jia, K. Hayat, J. Yu, S. Deng, E. Karangwa, E. Duhoranimana, S. Xia and X. Zhang, Controlled formation of flavor compounds by preparation and application of Maillard reaction intermediate (MRI) derived from xylose and phenylalanine, *RSC Adv.*, 2017, **7**, 45442–45451.

53 Y. Li, B. Jiang, T. Zhang, W. Mu and J. Liu, Antioxidant and free radical-scavenging activities of chickpea protein hydrolysate (CPH), *Food Chem.*, 2008, **106**, 444–450.

54 W. Wang, Y. Bao and Y. Chen, Characteristics and antioxidant activity of water-soluble Maillard reaction products from interactions in a whey protein isolate and sugars system, *Food Chem.*, 2013, **139**, 355–361.

